Chalcogenide Letters Vol. 22, No. 3, March 2025, p. 255 - 260

Synthesis and characterizations of Cu_2BaSnS_4 nanoparticles via solvothermal route

G. Hao *, Z. Chen, R. Xian, W. Yifan

School of Materials Science and Engineering, Yancheng Institute of Technology, 211 Jianjun East Street, Yancheng 224051, PR China

In present work, Cu_2BaSnS_4(CBTS) nanoparticles are reported solvothermally synthesized. The formation of single-phase trigonal structure of CBTS nanoparticles is confirmed by XRD and Raman spectroscopic analysis. SEM studies reveal that CBTS exhibits flower shaped structure self-assembling by nanosheets with uniform average thickness 30nm. CBTS materials show abroad absorption in the complete visible range, providing a band-gap value of 1.58eV, indicating potential applications in photocvoltaics. The excellent MB degradation efficiency of 93% under visible light within 100min is achieved, suggesting CBTS is a potential material for effective solar light photocatalytic application. Meanwhile, electrical properties are measured up to 675K, the value of Seebeck coefficient of CBTS material can reach to 111.42$\mu V \bullet K^{-1}$, meanwhile the value of electrical conductivity is 18.24$S \cdot m^{-1}$, indicating its potential for thermoelectric application.

(Received January 11, 2025; Accepted March 17, 2025)

Keywords: Semiconductors, Cu_2BaSnS_4, Nanocrystals, Solvothermal, Optical, Photocatalytic, Electrical transport

1. Introduction

In recent years, chalcogenide ternary and quaternary compounds has been actively pursued for thin-film solar cells, thermoelectric devices and other catalytic systems. As a *P*-type semiconductor material. Cu_2ZnSnS_4(CZTS) has been widely explored in previous some years due to an optimal band gap, high absorption coefficient and low lattice conductivity [1-4]. However, CZTS is facing anti-site defects for applications in different domains such as energy harvesting and photocatalysis, which result in carrier recombination, potential fluctuations and band tailing. One such material that analogous to CZTS based on optimal bandgap and absorption coefficient, Cu_2BaSnS_4(CBTS) is predicted to prevent the formation of anti-defects. In the past few periods, Cu_2BaSnS_4(CBTS) has been studied using theoretical and experimental research, which are mainly devoted to the development of solar cells [5-11].

In this work, we are focused on a solvothermal method to synthesize Cu_2BaSnS_4(CBTS) nanoparticles. Additionally, Cu_2BaSnS_4(CBTS) nanoparticles are characterized using X-ray powder diffractometer, Raman spectroscopy, scanning electron microscopy, UV-visible spectrophotometer and thermoelectric system to control structure, morphology, photocatalytic and electrical transport performances.

2. Experimental details

All analytical grade chemicals Copper chloride dihydrate [$CuCl_2 \cdot 2H_2O$], Barium acetate [$Ba(C_2H_3O_2)_2$], Tin(II) chloride dihydrate [$SnCl_2 \cdot 2H_2O$], and Thiourea [H_2NCSNH_2] are procured

* Corresponding author: guanhao1980@sina.com
https://doi.org/10.15251/CL.2025.223.255

from Sinopharm Chemical Reagent Co. Ltd. In order to synthesize Cu_2BaSnS_4(CBTS) nanoparticles, 0.341g $CuCl_2 \cdot 2H_2O$ (0.002M), 0.255g $Ba(C_2H_3O_2)_2$ (0.001M), 0.225g $SnCl_2 \cdot 2H_2O$ (0.001M) and 0.457g H_2NCSNH_2 (0.006M) are assimilated in appropriate amount ethylene glycol(EG) are constantly stirred for 2h to obtain a homogeneous solution, then the solution is taken in a autoclave with Teflon linnig and solvothermally treated at 200℃ for 24h. Next, the black solution is left to be cooled to room temperature naturally after the completion of reaction time. By washing several times with deionized water, the black products are dried under vacuum at 60℃ and are stored for further investigations. In order to study electrical transport properties, CBTS nanoparticles are utilized to prepare pellet samples under a pressure of 60MPa and sintering 500℃ for 1h in vacuum.

The phase structure of the synthesized sample is examined using X-ray powder diffraction (Rigaku

3. Results and discussion

The crystal structure of as-synthesized CBTS nanoparticles is proved by XRD from Fig.1. We can observe that all the prominent peaks at diffraction angles 19.73°, 23.32°, 28.11°, 32.45°, 37.87°, 52.53° and 48.27° are well indexed and assigned with the respective (102), (103), (104), (105), (203), (204) and (213) miller planes of trigonal structure (JCPDS no. 30-0124). Absence of the featured peaks from other crystalline forms indicate the formation of pure CBTS nanoparticles. The lattice constant values of CBTS nanoparticles are calculated to be a=b=6.3Å and c=15.8Å, which is in good agreement with that previous finding by others [12]. The main crystallize size of CBTS is founded to be 22.3nm estimated using Debye-Scherrer formula. It is noteworthy that XRD analysis cannot sufficient to differentiate among the similarity of the XRD patterns for some chalcogenides such as CBTS, Cu_2S, Cu_2SnS_3 and Cu_3SnS_4. Raman spectrum being further confirmed the structure is shown in the inset. The obvious characteristic peaks at 341cm^{-1} and 367cm^{-1} corresponding to the Raman vibration of CBTS nanoparticles are observed, which is well supported by the previous report [13]. The absence of the peaks at 475cm^{-1}(Cu_2S), 356cm^{-1}(Cu_2SnS_3) and 315cm^{-1} (Cu_3SnS_4) strong confirm single phase of CBTS nanocrystals.

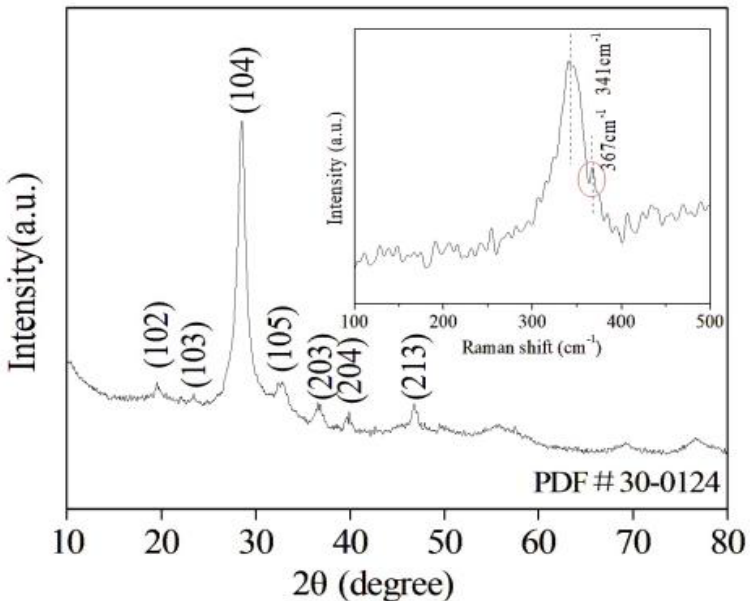

Fig. 1. XRD pattern of CBTS nanoparticles; Inset: Raman spectrum of CBTS nanoparticles.

The micro-morphology of as-prepared CBTS material is investigated. The sample exhibits nanoflower structure self-assembling by nanosheets as shown in Fig.2. The average size of uniform nanoflowers is about 3μm, while the average thickness of nanosheets is about 30nm. The flower structure with large areas helps in improving the catalytic efficiency by enhancing more absorption sites [14].

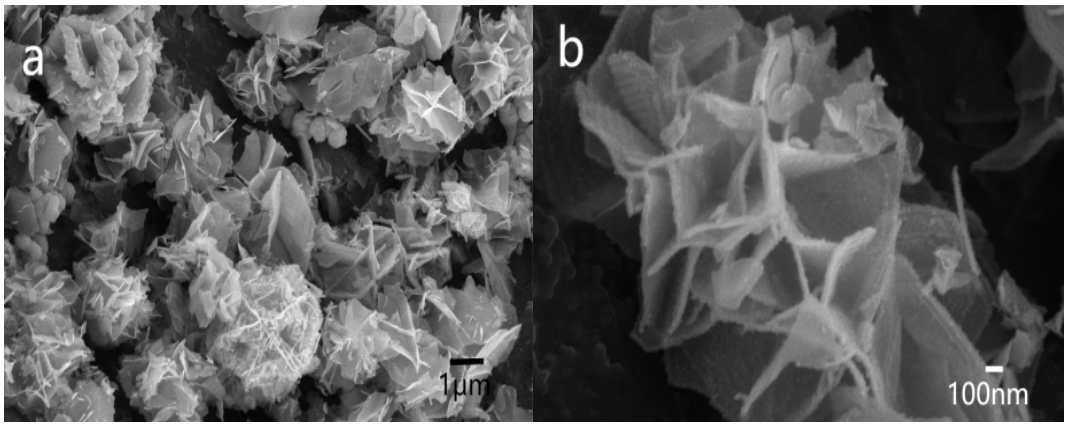

Fig. 2. Low magnification(a) and high magnification(b) SEM images of CBTS nanoparticles.

In order to find out the optical energy band-gap value of CBTS nanoparticles, UV-vis-NIR spectrum is recorded in the wavelength range 400-900nm, as shown in Fig.3. From the spectrum, it is clearly visible that CBTS nanoparticles exhibit abroad absorption in the complete visible part. The energy band-gap value of the prepared CBTS nanoparticles can be determined by an equation with hv as abscissa and $(\alpha hv)^2$ as ordinate. The inset shows a band-gap value about 1.58eV for CBTS nanoparticles, which agrees well with the previously reported [9].

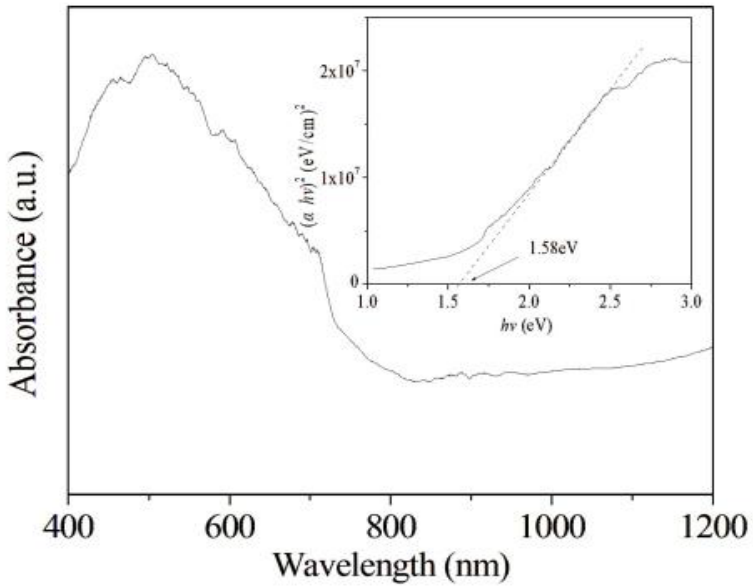

Fig. 3. UV-Vis spectrum of CBTS nanoparticles; Inset: Optical bandgap estimation of CBTS nanoparticles.

CBTS nanoparticles are explored for photocatalysis by examining the photocatalytic degradation of methylene blue(MB) under illumination of visible light on the condition of different time. The proportion is plotted against the illumination time shown in Fig.4(a) for MB treated with CBTS catalysts. It is found that flower shaped CBTS sample decolored about 93% of MB in 100min illumination. High surface area together with the presence of catalytically numerous active edge site is a major factor for high photocatalytic efficiency. The CBTS nanoparticles are used for three consecutive degradation cycles to explore their reusability. Furthermore, the structure after degradation is also observed to check their stability. As shown in Fig.4(b), the degradation efficiency only falls from 93% to 89% after three consecutive degradation cycles. And it is found from Fig.4(c) that there is hardly change in the pattern before and after the catalytic reactions. The results indicate excellent reusability and stability of CBTS nanoparticles during the photocatalysis.

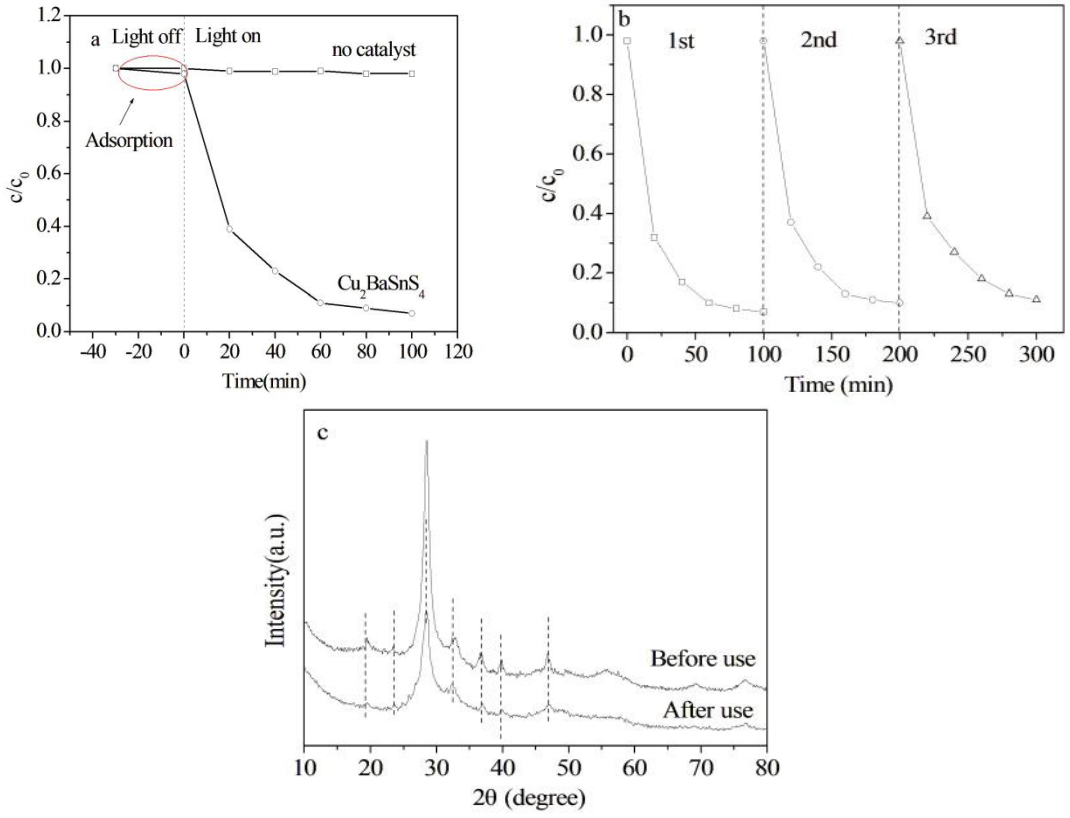

Fig. 4. (a)the efficiencies of degradation of MB as a function of different time (b) the photo stability of CBTS nanoparticles (c) the structural stability of CBTS nanoparticles.

Fig. 5 depicts the temperature dependence of Seebeck coefficient (*S*) and electrical conductivity (σ) of CBTS sample. The positive coefficient values exhibit *P*-type electrical transport behavior. The values of Seebeck coefficient and electrical conductivity of CBTS sample increase as the measured temperature increases. The value of Seebeck coefficient for CBTS sample is about 111.42μV•K^{-1} while it possesses a slightly higher value of electrical conductivity of 18.24S·m^{-1} at 675K.

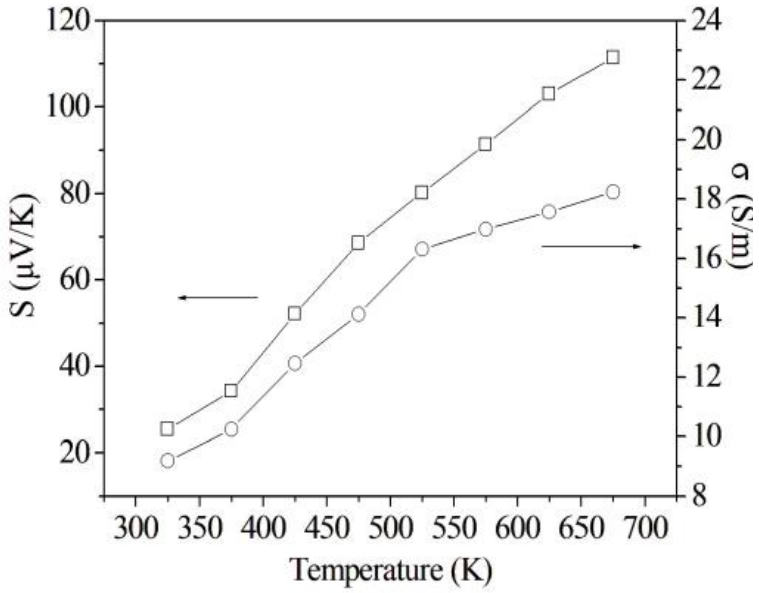

Fig. 5. Temperature-dependent plot of Seebeck coefficient and electrical conductivity of CBTS sample.

4. Conclusions

In the work, *P*-type Cu_2BaSnS_4 semiconductor material is effectively synthesized by a solvothermal approach. XRD and Raman spectroscopic studies corroborate the single-phase formation of the prepared CBTS nanoparticles. The morphology investigated by SEM reveals the flower like structure being composed of nanosheet with uniform average thickness 30nm. Cu_2BaSnS_4 nanocrystals with the narrow band gap of about 1.58eV remove 93% of the methylene blue(MB) in 100min under illumination of visible light, depicting a promise in treatment of water pollutants. The high value of Seebeck coefficient and moderate value of electrical conductivity of Cu_2BaSnS_4 sample are synthesized, which establishes that Cu_2BaSnS_4 is a promising material for typical thermoelectric application.

References

[1] B. D. Long, L. H. Thang, N. H. Hai, K. Suekuni, K. Hashikuni, T. Q. M. Nhat, W. Klich, M. Ohtaki, Mat. Sci. Eng. B-Adv. 272, 115353 (2021); https://doi.org/10.1016/j.mseb.2021.115353

[2] R. Henríquez, P. S. Nogales, P. G. Moreno, E. M. Cartagena, P. L. Bongiorno, E. Navarrete-Astorga, E. A. Dalchiele, Nanomaterial 1731, 13(2023); https://doi.org/10.3390/nano13111731

[3] S. Manjula, A. Sarathkumar, G. Sivakumar, J. Nano Research 79, 25 (2023); https://doi.org/10.4028/p-b6b546

[4] K. Gupta, S. Gupta, Y. Batra, Mat. Sci. Eng. B-Adv. 303, 117291 (2024); https://doi.org/10.1016/j.mseb.2024.117291

[5] R. Chakraborty, P. Ghosh, Appl. Surf. Sci. 570, 151049 (2021); https://doi.org/10.1016/j.apsusc.2021.151049

[6] S. P. Madhusudanan, E. Balamoorthy, S. Kumar M., T. G. Manivasagam, S. K. Batabyal, J. Solid State Electr. 26, 2411 (2022); https://doi.org/10.1007/s10008-022-05243-6

[7] M. V. Gapanovich, E. V. Rabenok, V. V. Rakitin, E. N. Koltsov, S. G. Protasova, D. M. Sedlovets, G. V. Shilov, A. V. Stanchik, V. F. Gremenok, M. I. Sayyed, D. I. Tishkevich, A. V. Trukhanov, J. Solid State Chem. 339, 124930 (2024); https://doi.org/10.1016/j.jssc.2024.124930

[8] S. Lie, M. Guc, V. Tunuguntla, V. Izquierdo-Roca, S. Siebentritt, L. Helena Wong, J. Mater. Chem. A 10, 9137 (2022); https://doi.org/10.1039/D2TA00225F

[9] A, Ziti, B. Hartiti, S. Smairi, H. Labrim, Y. Nouri, H. J. T. Nkuissi, A. Belafhaili, S. Fadili, M. Tahri, P. Thevenin, J. Mater. Sci.: Mater. Electron. 33, 24477 (2022); https://doi.org/10.1007/s10854-022-09160-2

[10] Y. Yan, B. Xia, Z. Xu, X. Wang, ACS Catal. 4, 1693 (2014); https://doi.org/10.1021/cs500070x

[11] B. Teymur, Y. Zhou, E. Ngaboyamahina, J.T. Glass, D.B. Mitzi, Chem. Mater. 30, 6116 (2018); https://doi.org/10.1021/acs.chemmater.8b02556

[12] A. Ali, S. Ahmed, J. Rehman, M. R. Abdullah, H. Chen, B. Guo, Y. Yang, Mater. Today Commun. 26, 101675 (2021); https://doi.org/10.1016/j.mtcomm.2020.101675

[13] H. Luo, J. Chen, X. Zhang, S. Wang, H. Gu, W. Wang, H. Li, Mater. Lett. 270, 127750 (2020); https://doi.org/10.1016/j.matlet.2020.127750

[14] A. Abbas, K. Li, X. Guo, A. Wu, F. Ali, S. Attique, A. Ahmad, Environ. Res. 205, 112539(2022); https://doi.org/10.1016/j.envres.2021.112539